Chapter 3

Adsorption and abstraction of atomic hydrogen on the Si(110) surfaces

As was mentioned in Chapter 1, when D/Si surfaces are exposed to atomic H beam, HD and D_2 molecules are desorbed from the surface. To reveal the H reaction kinetics and dynamics, several groups have studied adatom abstraction on Si surfaces. Recently proposed hot-complex (HC) model can explain successfully the ABS and AID pathways on the Si(100) and Si(111) surfaces. In contrast, D abstraction by H on Si(110) surface has been less studied.[1]

In this chapter, I have studied kinetic mechanism of D abstraction by H on the saturated and unsaturated D/Si(110) surfaces. Surface species formed during the exposure of H atoms may play a vital role in AID pathways. These species are illuminated by FTIR and TD spectroscopies. In detailed analysis of measured HD and D_2 rate curves, I have found that the H-induced desorptions from D/Si(110) surfaces are quite nonlinear with respect to D coverage. Net HD and D_2 desorption rate curves are fitted with proposed rate equations. Activation energies for ABS and AID are measured from Arrhenius rate constants determined by curve fitting. Based on these results, mechanisms of the ABS and AID reactions on the Si(110) surface are proposed in the light of HC model and comparatively discussed with those on Si(100) surfaces, for the first time.

3.1 Experiment

Details of experiment have been explained in Chapter 2. Here only the preparation method of unsaturated and saturated D covered Si(110) surface, rotation speed of beam chopper and FTIR are described. For abstraction experiments, the clean Si(110) surface was first exposed to D atoms to prepare D-covered surface. Two different ways were employed for D coverages, controlling D exposure time and surface temperature. D-saturated surfaces were prepared by 5 min D dosing at a set of temperatures to reveal the *T*s dependence of abstraction. In experiments for Ts > 523 K, to minimize loss of D adatoms due to desorption before H exposure, I employed a quick heating of the sample within 1.5 s from D dosing temperature of 523 to 573 K or 623 K. In this case, H exposure was started coincidentally with the quick sample heating. Hence, it is reminded that the D-saturated surfaces contain dideuterides before H exposure. On the other hand, 1 ML D-covered Si surface was prepared by 2 min D exposure at 523 K, where dideuterides are unstable due to β_2 TD. Thus, this surface does not contain any dideuterides, and is referred to as unsaturated surface. Pulsed H-beam with 0.5s on-and 9.5s off-cycles was used. Signal pulses from the QMS were fed into a multi-channel scalar (1024 channel, dwell time of 9 ms) triggered with the rotating chopper. Infrared (IR) spectra of H-terminated Si(110) surfaces were obtained with the FTIR absorption spectrometer in an ultra high vacuum chamber as was mentioned in section 2.6. IR spectrum measured for the clean Si(110) surface was used as a background. Deposition of H atoms onto the sample was done through thermal cracking of H_2 gas on a heated W filament.[2]

3.2 Various surface species

Surface species of monodeuterides and dideuterides on the D/Si(110) surface must be confirmed before starting the kinetics study of the H induced HD and D_2 desorption from the surfaces. These species are confirmed by the room temperature FTIR and thermal desorption spectroscopy (TDS).

3.2.1 FTIR spectra

IR spectra of the H-terminated Si(110) surface were measured with an unpolarized light. The RHEED patterns showed a well ordered (16x2) structure on the clean Si(110) surface, and diffuse (1x1) structure on the surface terminated with H atoms after 3000 L H_2 exposure. The IR absorption spectrum was measured on the H-terminated surface at room temperature and was plotted in Fig.3.1. There are four characteristic absorption peaks at 2070, 2084, 2099 and 2135 cm^{-1}. The intense 2070 and 2084 cm^{-1} peaks are attributed to the out-of-phase and in-phase stretching vibration of monohydrides, respectively. The 2099 cm^{-1} peak could be attributed to the Si–H stretching vibration originated from surface adatoms or hydrides at defect sites.[3] The peak at 2135 cm^{-1} is due to the dihydrides.[4] According to Shinohara *et.al.*, dihydrides on the Si(110) surfaces are formed by breaking either the topmost –SiH–SiH– zigzag chain or the Si–Si bond between the first and second Si layers. As will be discussed in later subsections, the dihydrides may play a key role in the AID reaction.

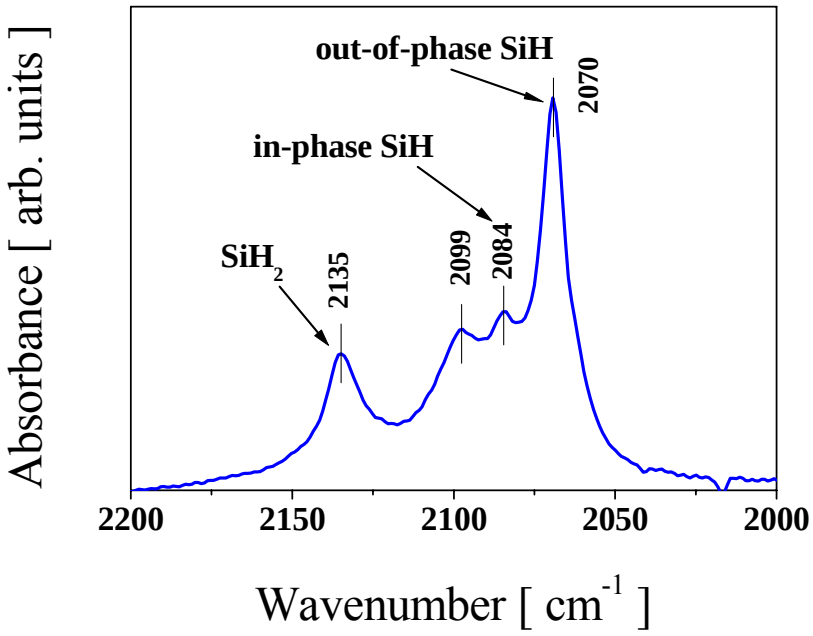

Fig. 3.1 Infrared absorption spectra in the Si–H stretching vibration region of the Si(110) surface recorded after 3000 L H_2 exposure at room temperature.

3.2.2 Thermal desorption (TD) of D_2

To reconfirm the surface entities by the thermal desorption (TD) spectroscopy, the clean Si(110) surface was exposed to D atoms at 373 K to prepare D-precovered surfaces. D-precoverages, θ_D^0, were changed by controlling D exposure time and determined from TD spectra. Fig.3.2 shows the TD spectra measured on the D/Si(110) surfaces for various θ_D^0. For $\theta_D^0 > 1$ ML, the β_2 peak around 600 K can be attributed to surface dideuterides[5] On the other hand, for a very small value of θ_D^0, the peak depicted as β_1 has a maximum at around 800 K, being attributed to the surface monodeuterides. The β_1 peak shifted to a lower

temperature region (~750 K) with increasing θ_D^o as shown by the dashed curve, suggesting that TD obeys a second-order rate law.[5] The β_1 peaks look asymmetric in spectral line shape. According to Kim, two different types of monohydrides could be involved there. One should note that there is no existence of α-peak at around 960 K,[6] suggesting no D atoms are taken into the subsurface layers. This was also reported in the literature.[5] Atomic D incorporation into the subsurface layers could be promoted by surface roughness created by Ar^+ sputtering or by H(D)-induced surface etching.

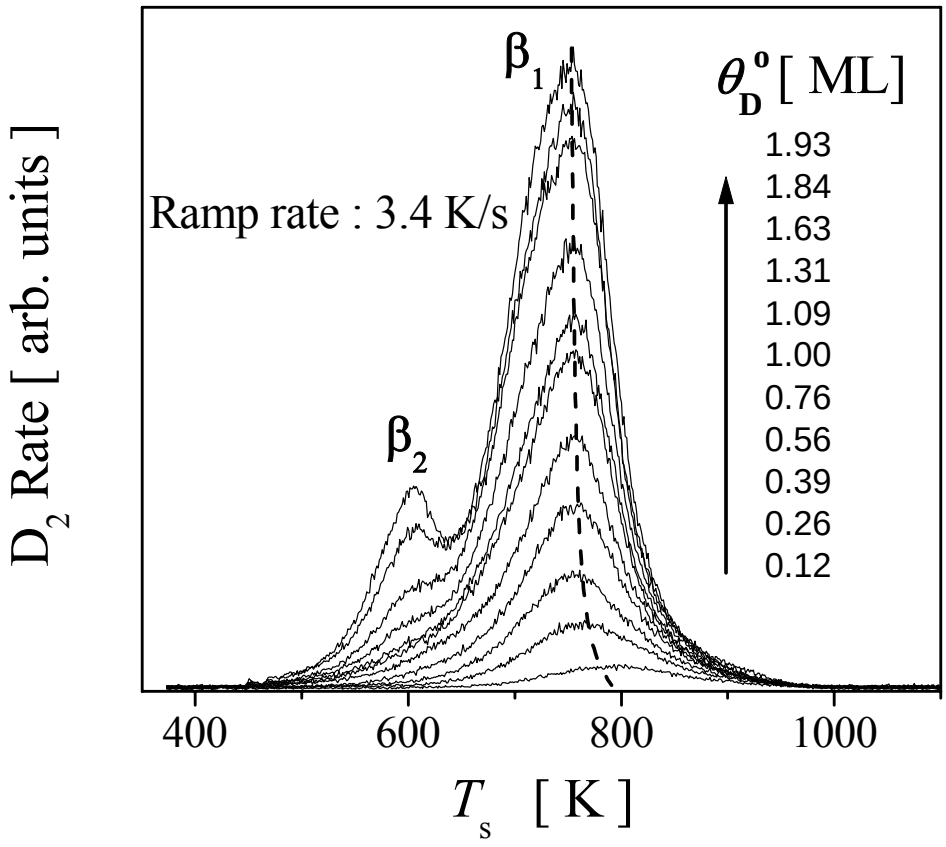

Fig. 3.2 D_2 thermal desorption (TD) spectra from the Si(110) surface as a function of initial D coverages. β_2: TD arising from the di-deuteride phase. β_1: TD arising from the monodeuteride phase. The dashed line shows the systematic peak shift which suggests a second order desorption kinetics. The D/Si(110) surface was prepared at 373 K.

3.3 D uptake curve

Prior to abstraction experiments, we measured uptake of D atoms on the clean Si(110) surface as a function of exposure time t at 523 K. Uptake of D adatoms was evaluated from TD spectra measured for various exposure times. Figure 3.3 shows D uptake curve measured at 523 K as a function of time. One may find that the uptake curve is about linear at the early stages of D exposure. On the other hand, the rate of D uptake tends to be level off after sufficient D exposure. This feature would suggest that the sticking coefficient of D atoms might be small on the D-terminated surfaces. However, one should remind that such a decrease in the sticking coefficient is nominal since surface D abstraction by incident D followed by quick resupply of adatoms is involved there. In later subsections, this will be clearly seen as D abstraction by H.

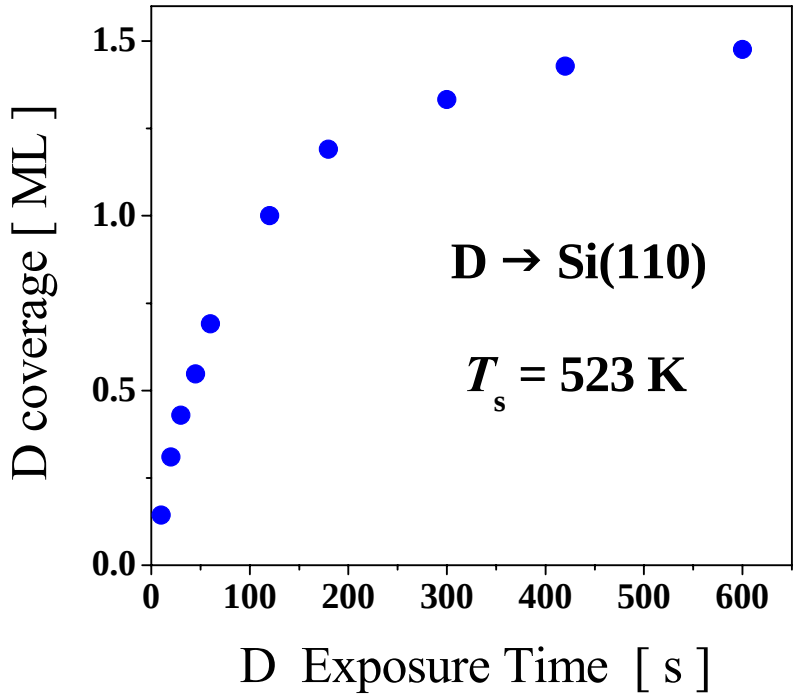

Fig. 3.3 D uptake curve measured at 523 K on the clean Si(110) surface.

3.4 H-induced reactions on D/Si(110)

In order to reveal the reaction kinetics of H induced HD and D_2 desorptions from D/Si(110) surfaces, saturated and unsaturated surfaces were prepared. Here by saturated, I mean that the surface contains dideuterides and by unsaturated I mean dideuterides free surfaces. These surfaces are subjected to direct atomic H beam at various *T*s. During exposure of D/Si(110) surfaces to H atoms, HD and D_2 molecules were found to desorb as detected by the QMS. D_2 and HD rate curves measured at various *T*s on saturated and unsaturated surfaces were plotted in Fig.3.4 and Fig.3.5, respectively. Immediately after the start of H exposure, both HD and D_2 rate curves step up at H exposure time, t = 0. On the D-saturated surfaces, then they decay almost exponentially with time due to loss of D adatoms via abstraction reactions. On the other hand, on the unsaturated surface, the maximum of the peak apparently lags. This means that, at t=0, there is a rapid rate jump, but it still increases further to a peak maximum and then decreases exponentially. With increasing *T*s, the peak maximum shifts to the shorter time region. The *T*s dependent peak shift is caused not only by direct ABS but also by adsorption-induced desorption (AID) occurring among D adatoms and H adatoms. The reason is that H adatoms are gradually piled up during the H exposure and HD is formed through the AID paths.

In contrast to the HD desorptions, the observed D_2 desorption exhibits a strong *T*s dependence on both saturated and unsaturated surfaces. No D_2 desorptions are observed at 373 K. However, at temperatures higher than 500 K where β_2 TD is activated, D_2 AID becomes facile. For *T*s > 573 K where β_1 TD partially occurs as shown in Fig. 3.2, a sharp peak appears at around t = 0. This sharp peak is not due to H-induced desorption but due to nonequilibrium TD induced by the very quick temperature rise. Nascent D_2 desorption induced by H can be analyzed in the time region after this sharp peak. The rates of AID were

much higher than that of TD for the temperature region studied in this work.

An induction time can be recognized for the D_2 desorption at 473 and 523 K on the unsaturated surface as shown in Fig. 3.4 (will be clearly seen in Fig.3.9). If this induction time is added by 2 min for the preparation of 1 monolayer (ML) precoverage, considerable amount of dihydrides must be excessively formed after the induction time. Hence the induction time may be correlated to the H exposure time needed for the surface saturation. In another words, induction time is necessary to form surface dideuterides (dihydrides) on the 1ML D/Si(110) surfaces.

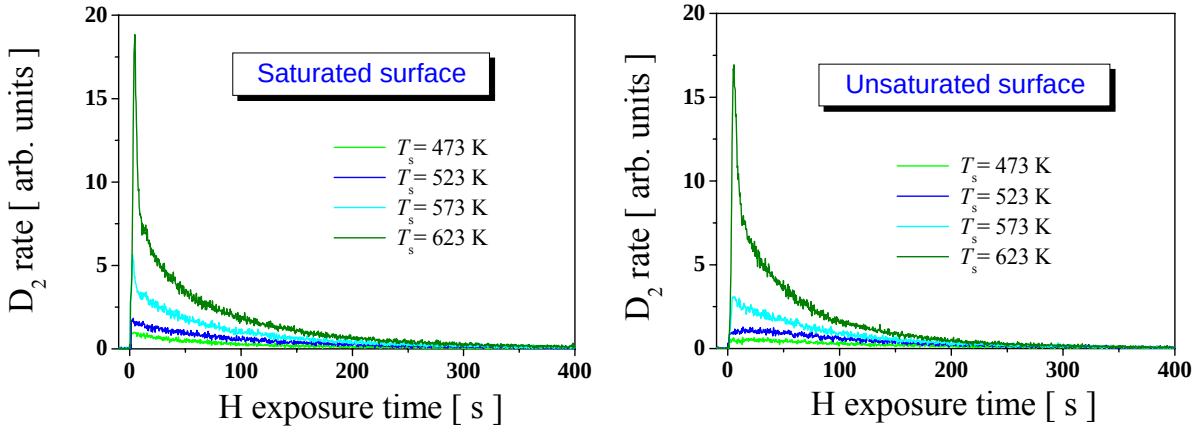

Fig. 3.4 Plots of D_2 rate curves as a function of H exposure time on saturated and unsaturated surfaces at different Ts. No D_2 desorption was observed at *T*s = 373 K.

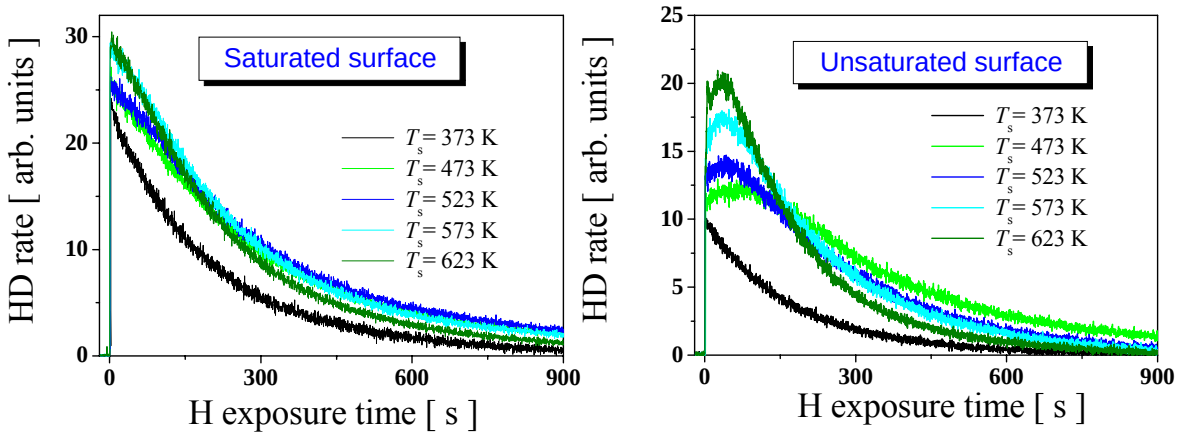

Fig. 3.5 Plots of HD rate curves as a function of H exposure time on saturated and unsaturated surfaces at different *T*s.

3.5 Analysis of HD and D_2 rate curves

3.5.1 Proposed rate equations

The observed feature of the H-induced D_2 and HD desorptions from the D/Si(110) surfaces looks similar to that on the Si(100)[7,8,9] or Si(111)[10] surfaces, where a second and nearly fourth- or third-order kinetics have been recognized for ABS and AID, respectively. In order to estimate the AID and ABS reaction orders on the Si(110) surface, the measured D_2 and HD rate curves were first fitted to a single term rate equations shown below:

$$R_{D_2} = k\,\theta_D^m \qquad \text{and} \qquad R_{HD} = c\theta_D^m$$

where R_{D2} and R_{HD} are the D_2 and HD desorption rate, respectively. As a result, it turned out that the fourth- and second-order rate laws are operative for AID and ABS, respectively. On the basis of the evaluated values for the reaction orders, the D_2 and HD rate equations proposed for the Si(100) surface[7] are employed for more detailed analysis of the measured rate curves. First, we construct a D_2 rate equation which consists of only AID terms. As mentioned above the AID reaction obeys a fourth-order rate law in θ_D and θ_H, which implicate that four adatoms are necessary as a target of an H atom for AID. For such a mixed phase of H and D adatoms, three possible configurations for four adatoms are now referred to as 4D, 3D1H, and 2D2H configuration. Here the 4D, 3D1H, and 2D2H configurations contain four D adatoms, three D and one H adatom, and two D and two H adatoms, respectively. From the analogy to the AID mechanism proposed on the Si(100) surface,[11] we tacitly assume that two adatoms among the four adatoms are on a same Si dideuteride and the other two adatoms are on two monodeuterides. Here the both species are adjacent to each other on a zigzag Si chain. The rate equation for the D_2 desorption is thereby written as

$$R_{D_2} = \eta(t)[k_1\theta_D^4 + k_2\theta_D^3\theta_H + k_3\theta_D^2\theta_H^2], \qquad (4)$$

where,
$$\eta(t) = \frac{1}{2}\left[1 + erf\left(\frac{\theta_{H+D}(t) - \upsilon_D^o}{\omega(\theta_D^o)}\right)\right]. \qquad (5)$$

Here, k_i (i = 1, 2, 3) are the rate constants. The function $\eta(t)$ gives time evolution of surface area at which AID can take place, being related to the observed induction time for AID. It is an s-shaped curve characterized with the threshold coverage υ^o_D and the width $\omega(\theta^o_D)$. In case of the Si(100) surface, (3 x 1) dihydride/monohydride domains were considered for such surface area. I think that on the Si(110) surface, the situation should be similar. This is because, the desorption rate on the saturated surfaces, as shown in Fig. 3.4. (left), no induction times were present for the surfaces already saturated with dideuterides before H exposure. Hence, for the saturated surfaces it can be set that $\eta(t)$ = 1.0. On the other hand, on the unsaturated surface, the peak maximum obviously timely lags at 473 K and 523 K as shown in Fig. 3.4.(right), or will be more clearly seen in Fig. 3.9. This time lag in the peak of the D_2 rate curve is caused by the delay in the surface saturation during H exposure.

Now we are going to propose a HD rate equation. The AID channels must be involved even in the HD desorption as H adatoms are piled up during H exposure. Considering this contribution of AID into account, the HD rate equation can be written as follows:

$$R_{HD} = c_1\theta_D^2 + \eta(t)[c_2\theta_D^3\theta_H + c_3\theta_D^2\theta_H^2 + c_4\theta_D\theta_H^3] \qquad (6)$$

Here, c_i (i = 1, 2, 3, 4) stands for the intensity which includes the H flux as well as the rate constant for each desorption pathway. The function, $\eta(t)$, is again used for the AID term but not for the ABS term. The 1D3H situation which contains one D and three H adatoms is newly added in Eq. (6).

3.5.2 D and H coverages during H exposure

In the proposed rate equations, the net D_2 and HD desorption rates are functions of $\theta_D(t)$ and $\theta_H(t)$ coverages. These D coverages at t were evaluated from the measured HD and D_2 desorption rate and the TD spectra as follows,

$$\theta_D(t) = \int_t^{t_m} [R_{HD}(t) + 2R_{D_2}(t)]dt + \theta_D(t_m)\,. \qquad (7)$$

Here, $\theta_D(t_m)$ is the D coverages at t_m when abstraction experiments are stopped, and basically determined by TD. R_{HD} and R_{D2} are the desorption rate of HD and D_2. Considering the slow D uptake after the 1 ML D coverage as plotted in Fig. 3.3, the total H and D coverage under H exposure was assumed to increase linearly with time, shown in equation (8).

$$\theta_{D+H}(t) = \theta_D^o + \frac{\theta_D^f - \theta_D^o}{t_d} \times t \quad \text{-------} \quad (8)$$

Where, $\theta_D^{\mathbf{f}}$ is the final D coverages after t_d = 900s D dosing. Two examples of total coverages during H irradiation at 523 K on the saturated and unsaturated surfaces are shown in Fig. 3.6.

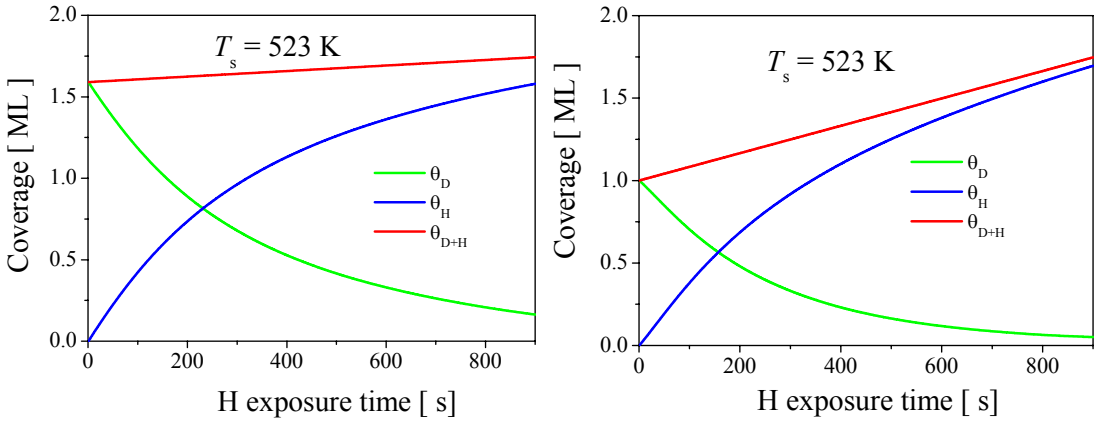

Fig. 3.6 Momentary coverages of D (θ_D, green line) and H (θ_H, blue line) on saturated (left) and unsaturated surface (right) at 523 K. The red lines represent the total coverages of H and D (θ_{D+H}).

3.5.3 Fitting of rate curves

In analyzing the measured rate curves with Eqs. (4) and (6), I begin with the saturated surface where $\eta(t) = 1$. All the D_2 desorption rate curves obtained at different Ts are smoothly fitted with the proposed rate equation (4) and decomposed into three components arising from the 4D, 3D1H, and 2D2H configurations. Fig. 3.7 shows fit results of the D_2 rate curve measured at different Ts.

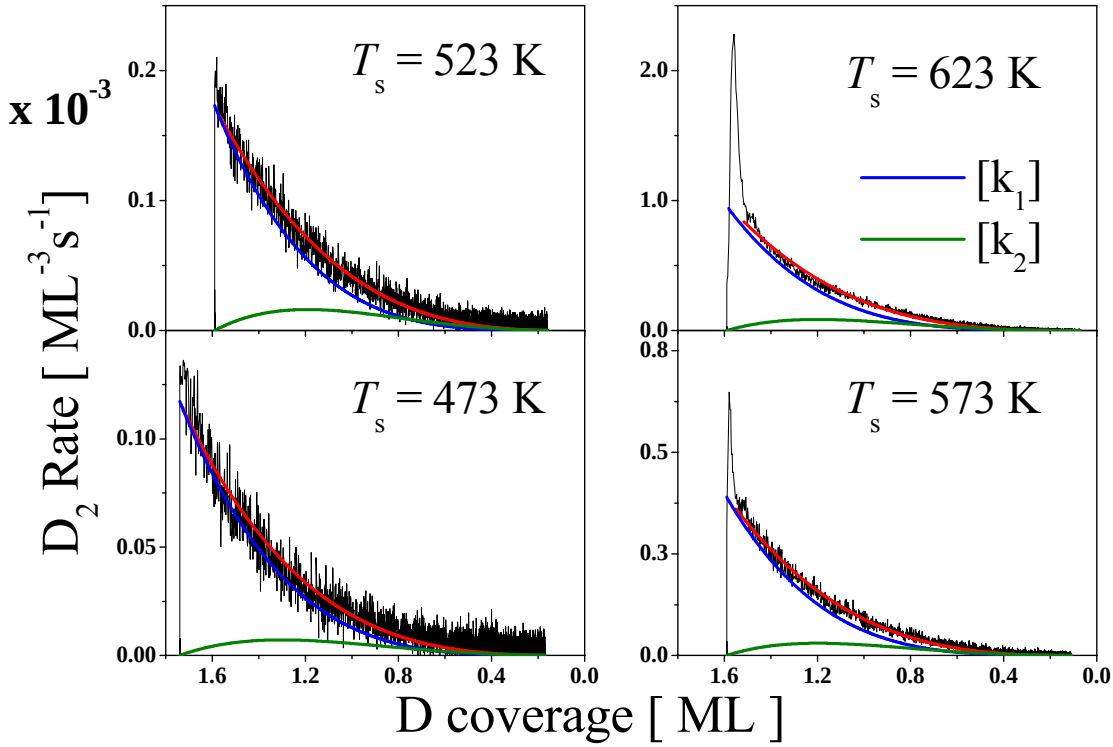

Fig. 3.7 Decomposition of the D_2 rate curves (black lines) measured on saturated surfaces at different Ts by best curve fitting (red lines) to the D_2 rate equation (4) in the text. The blue and green lines are $[k_1] = k_1\theta_D^4$ and $[k_2] = k_2\theta_D^3\theta_H$ terms respectively. On this saturated surfaces η=1. The values of rate constants k_i (i=1,2,3) are shown in the table 3.1.

For all the D_2 rate curves obtained on the saturated surfaces, we found that the 4D configuration mainly contributes to D_2 AID. The D_2 desorption tends to decrease with decreasing number of D adatoms in the configurations. The 2D2H configuration indeed

hardly contributes to D_2 AID. As will be discussed later, HD AID competes with the D_2 AID for the same 3D1H or 2D2H configuration.

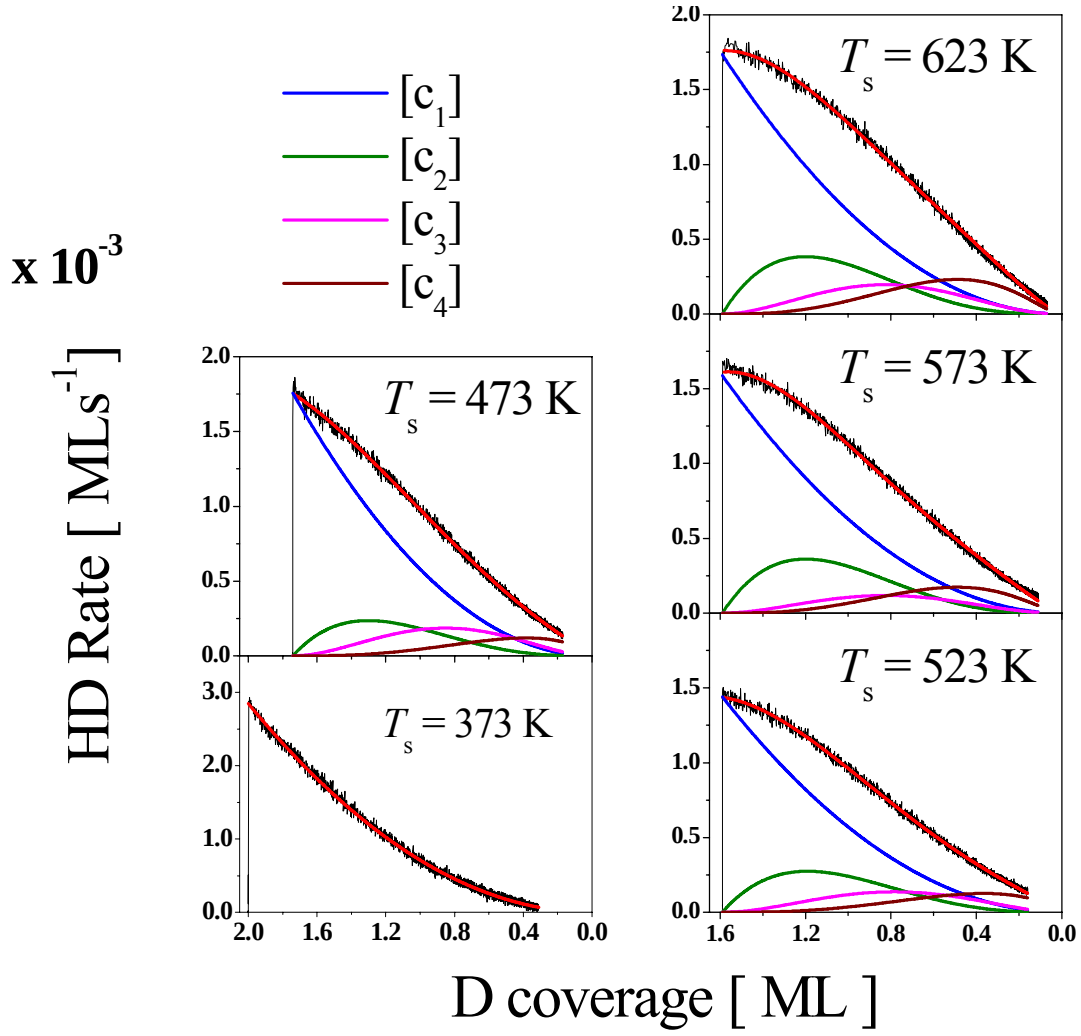

Fig. 3.8 Decomposition of the HD rate curves (black lines) measured on saturated surfaces at different *T*s by best curve fitting (red lines) to the HD rate equation (6) in the text. The blue, green, pink and wine color lines are $[c_1] = c_1\theta_D^2$, $[c_2] = c_2\theta_D^3\theta_H$, $[c_3] = c_3\theta_D^2\theta_H^2$ and $[c_4] = c_4\theta_D\theta_H^3$ terms respectively. On this saturated surfaces η=1. The values of rate constants c_i (i=1,2,3,4) are shown in the table 3.2.

The HD rate curves measured on the saturated surfaces were fit to Eq. (6) under the condition of $\eta(t)$ = 1. Fig. 3.8 shows results of decomposition of the HD rate curves measured at different *T*s. At 373 K, the lowest temperature in this study, the HD desorption arises solely along the ABS path but not along any AID paths. This result is consistent with the fact that no D_2 desorptions take place at this temperature as shown in Fig. 3.7. On the other hand, at temperatures higher than 473 K, the HD rate curves are contributed by both ABS and AID channels. Although the HD desorptions predominantly proceed via ABS channel, the total yield along the three AID channels is approximately equal to that along the ABS channel.

Rate constants of D_2 and HD reactions measured on saturated surface are summarized in the tables below at different *T*s.

Table: 3.1 Rate constants of D_2 desoprtion on the saturated D/S(110) surfaces

Temp, K.	k_1, $ML^{-3}s^{-1}$ x 10^{-5}	k_2, $ML^{-3}s^{-1}$ x 10^{-6}	k_3, $ML^{-3}s^{-1}$
373	--	--	--
473	1.28	7.0	0.0
523	2.71	23	0.0
573	6.1	50	0.0
623	15	140	0.0

Table: 3.2 Rate constants of HD desorption on the saturated D/Si(110) surfaces

Temp, K.	c_1, MLs^{-1} x 10^{-4}	c_2, $ML^{-3}s^{-1}$ x 10^{-4}	c_3, $ML^{-3}s^{-1}$ x 10^{-4}	c_4, $ML^{-3}s^{-1}$ x 10^{-5}
373	5.1	0.0	0.0	0.0
473	5.8	2.3	2.8	9.0
523	5.7	3.9	3.1	15
573	6.28	6.0	3.9	47
623	6.86	6.3	6.4	61

From the comparison of rate constants between c_2 and k_2 (the value is $3.9x10^{-4}$ ML^{-3} s^{-1} and $0.23x10^{-4}$ ML^{-3} s^{-1} at 523 K, respectively), we can extract a possible isotope effect on the HD and D_2 AID generated in the same 3D1H configuration. Since $c_2 > k_2$, HD AID takes place more efficiently than D_2 AID. Isotope effect may lead to a preferred association between lighter adatoms than heavier one due to quantum effects on, e.g. potential energy barriers that could be lowered by an amount of zero-point vibrational energy, tunneling probabilities through reaction barriers, or attempting frequency factors for access to transition states. Such a quantum effect on nuclear displacement predicts that the lighter atom can be superior to the heavier one for such a transition from atomic to molecular state.

In contrast to the saturated surfaces, D_2 and HD rate curves obtained on the unsaturated surfaces are characterized with induction times. They are again analyzed with Eqs. (4) and (6), respectively, taking the contribution from $\eta(t)$ into account. Fig.3.9 for D_2 molecules shows results of the best curve fit to Eq. (4). The delayed peak of the D_2 rate curve measured at 473 K and 523 K can be reproduced with $\eta(t)$ for the values shown in the table 3.3.

Table 3.3 Parameters to evaluate the $\eta(t)$.

Temp, K	υ_D^o [ML]	$\omega(\theta_D^o)$ [ML]
473	**1.002**	**0.013**
523	**0.998**	**0.013**

The induction time in AID is discernible for the 4D configuration or the curve [k_1] in Fig.3.9. At the beginning of H exposure, the surface does not contain any dihydrides. As was discussed before, AID requires presence of (–DSiD–) or (–DSiH–). For θ_D^o = 1 ML, building up such dihydrides on the surface is started at the initial stages of H exposure, giving rise to the induction time. This is also the case for HD AID since as shown in Fig. 3.10, a clear peaking at t > 0 can be seen in the measured rate curves on the unsaturated surfaces.

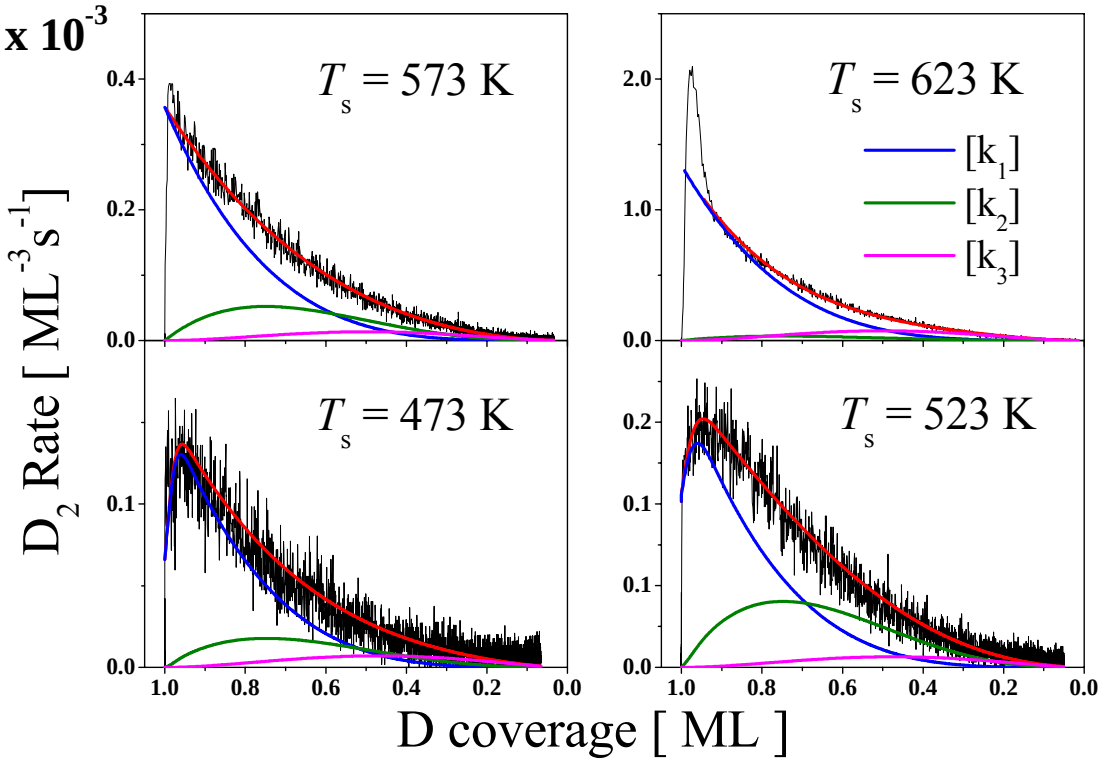

Fig. 3.9 Decomposition of the D_2 rate curves (black lines) measured on unsaturated surfaces at different *T*s by best curve fitting (red lines) to the D_2 rate equation (4) in the text. The blue , green and pink lines are $[k_1] = \eta k_1 \theta_D^4$, $[k_2] = \eta c_2 \theta_D^3 \theta_H$ and $[k_3] = \eta k_3 \theta_D^2 \theta_H^2$ terms respectively. The values of rate constants k_i (i=1,2,3) are shown in the table 3.4.

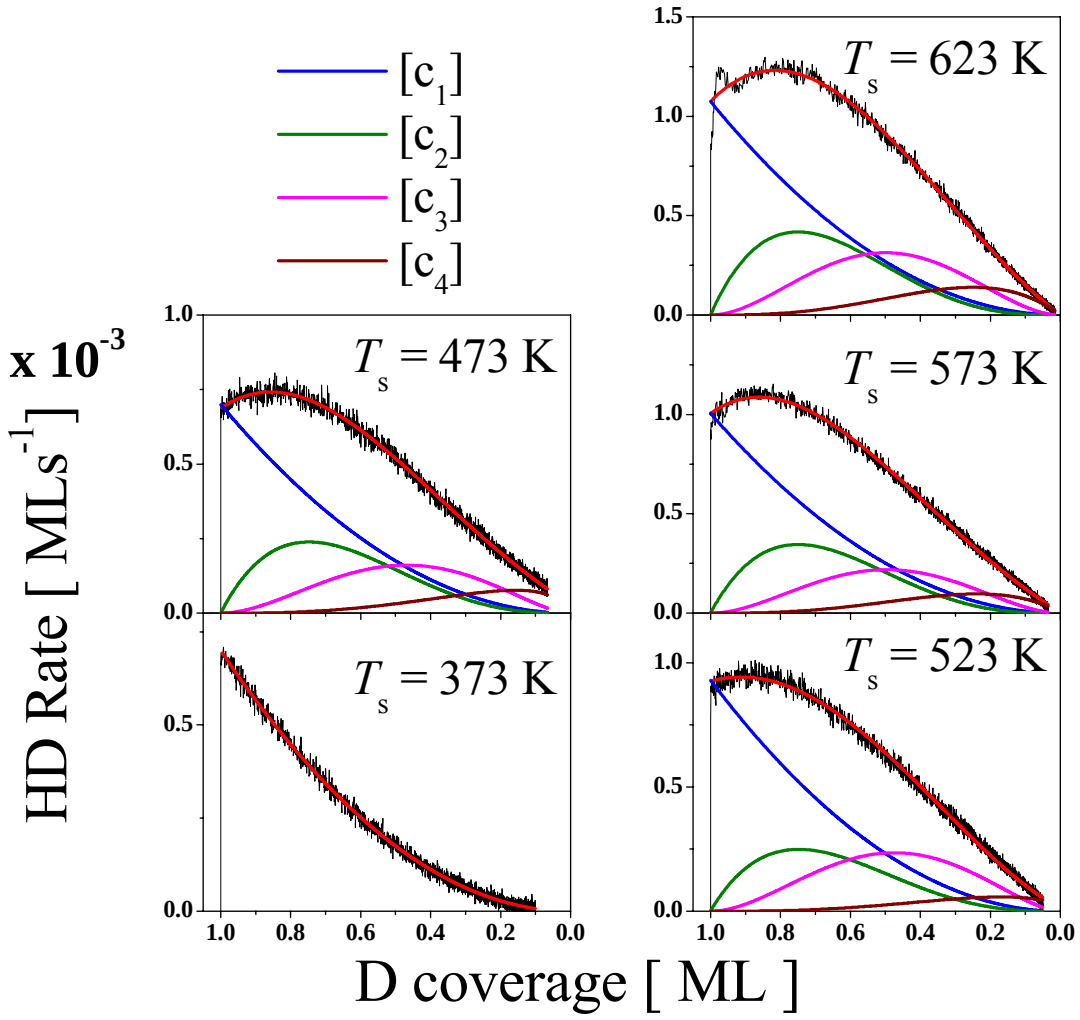

Fig. 3.10 Decomposition of the HD rate curves (black lines) measured on saturated surfaces at different Ts by best curve fitting (red lines) to the HD rate equation (6) in the text. The blue, green, pink and wine lines are

$[c_1] = c_1\theta_D^2$, $[c_2] = \eta c_2 \theta_D^3 \theta_H$, $[c_3] = \eta c_3 \theta_D^2 \theta_H^2$ and $[c_4] = \eta c_4 \theta_D \theta_H^3$

terms respectively. The values of rate constants c_i (i=1,2,3,4) are shown in the table 3.5

Table: 3.4 Rate constants of D_2 desorption on the unsaturated D/Si(110) surfaces

Temp, K.	k_1, $ML^{-3}s^{-1}$ x 10^{-5}	k_2, $ML^{-3}s^{-1}$ x 10^{-5}	k_3, $ML^{-3}s^{-1}$ x 10^{-5}
373	--	--	--
473	7.97	5.8	2.5
523	17.3	30	6.0
573	35.7	48	20
623	120	32	119

Table: 3.5 Rate constants of HD desorption on the unsaturated D/Si(110) surfaces.

Temp, K.	c_1, MLs^{-1} x 10^{-4}	c_2, $ML^{-3}s^{-1}$ x 10^{-3}	c_3, $ML^{-3}s^{-1}$ x 10^{-3}	c_4, $ML^{-3}s^{-1}$ x 10^{-4}
373	7.0	0.0	0.0	0.0
473	7.0	1.56	1.12	1.0
523	9.3	1.85	2.17	1.8
573	10.05	3.18	3.27	9.0
623	10.75	3.96	5.01	1.32

3.6 Activation energies

In order to evaluate activation energies E_a for ABS and AID, we make Arrhenius plots of c_1 and k_1 in Fig.3.11. The slopes of the curves yield $E_a = 0.06 \pm 0.01$ eV for HD ABS, and $E_a = 0.43 \pm 0.06$ eV for D_2 AID. The activation energy of 0.06 eV for ABS is just equal to that on Si(100).[9] Such a low activation energy suggests that the desorption along ABS is really direct in nature. The physical origin of such small activation energy in ABS may be related to vibrational excitation of the Si-D bond, since Koleske *et.al.*[12] calculated that ABS probability becomes higher with vibrational excitation of the Si–D bonds. On the other hand, the activation energy of 0.43 eV evaluated for AID is somewhat larger than that for ABS. This value is close to the values reported for AID on the Si(100) surface (0.2 eV [9]), with a certain deviation towards a larger value, however. This will be discussed in the next section.

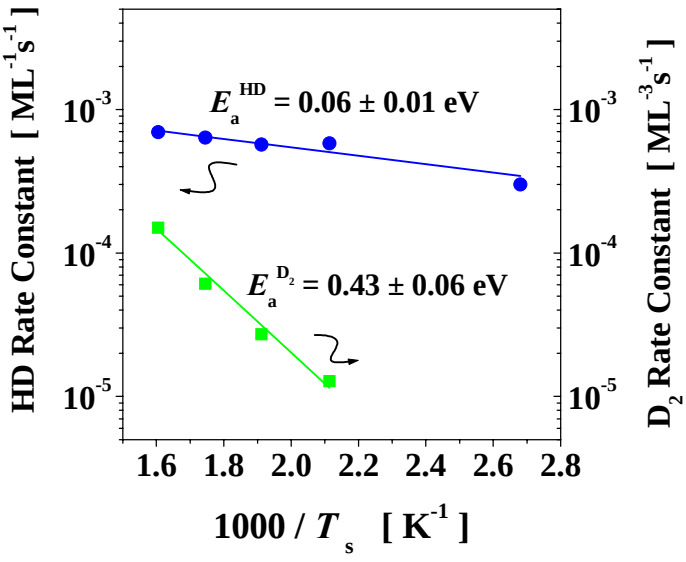

Fig. 3.11 Arrhenious plot of HD and D_2 desorption rate constants, c_1 for ABS and k_1 for AID determined by the best curve fitting method for the rate curves obtained on the D saturated Si(110) surface. The evaluated activation energies are written in the figure.

3.7 Time response of D_2 and proposed mechanism

In order to know the dynamical behavior of the ABS and AID reactions, we study the desorption behavior of HD and D_2 molecules by exposing the saturated D/Si(110) surface to modulated H beam with 0.5s on- and 9.5s off-time cycles at 573 K. Fig. 3.12 shows the measured transients desorption of D_2 and HD (inset) molecules. Desorption of D_2 is noted to be fast since its line shape is more or less similar to the incident H impulse (not shown). However, the time profile shows a somewhat slow rising and a tailing. This is obvious in comparison with the time profile of HD molecules that is quite prompt as shown in the inset. The fast desorption of HD molecules implicates that the main HD desorption occurs along the ABS path, consistent with its direct nature as confirmed in the extremely low activation energy of 0.06 eV as determined in Fig.3.11. Therefore, it is concluded that while the ABS process is fast, the AID process comprises from both a fast and a slow channel.

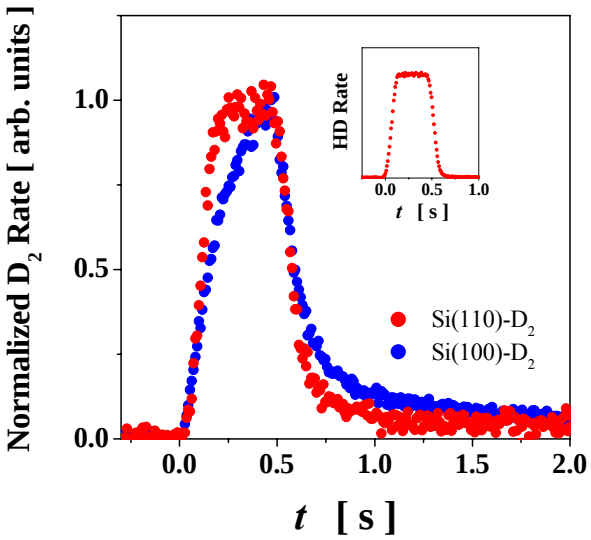

Fig. 3.12 Plots of transient D_2 desorption induced by the pulse H beam at 573 K. The transient desorption of D_2 molecules on the Si(100) surface is also reported for comparison. The rising and tailing parts of the two curves are different. The inset shows the HD desorption rate on the Si(110) surface. The ABS is quit prompt in nature.

Taking into account the second-order kinetics in θ_D and the prompt desorption of HD molecules, likely to the case on the Si(100) or Si(111) surfaces, the HC mechanism may be invoked to play a role in the ABS reaction. Fig. 3.13 shows a model of the HC on the Si(110) surface to illustrate the ABS. To explain not only the ABS but also the AID process, we consider a surface mixed with dideuterides and monodeuterides. Since structure of dideuterides (dihydrides) on the Si(110) surface has not been established, we here tacitly assume that dihydrides are formed in the backbonds of zigzag Si chains. The local structure of –DSi–SiD– is similar to a doubly occupied Si dimer DSi–SiD on Si(100) surfaces. An incident H atom is first trapped in an excited state of vibration in the chemisorption potential at a cell of –DSi–SiD–. During energy relaxation process, the H atom in the HC abstract one of the two D adatoms to generate HD ABS. If one of the two adatoms is H, the H atom of the HC may preferentially abstract the H adatom rather than the other D adatom because of an isotope effect. Therefore, to generate HD ABS the target must be bonded with two D adatoms, which causes the second-order kinetics with respect to θ_D. The lifetime of the vibrationally excited state determines reaction time for ABS, being expected shorter than a few ns[13] If ABS is skipped form the energy relaxation, the Si–Si bond or a Si backbond may be broken to make a dihydride, which would play a role in AID as will be discussed below.

Generation of AID along the fast and slow channels has also been found on the Si(100) surface.[11,14,15] The transient desorption of D_2 molecules measured on the Si(100) surface [14] is also replotted in Fig. 3.12 for comparison. One may notice that on the Si(110) surface, the contribution from the slow component is relatively smaller than that on the Si(100) surface. As was reviewed in the Chapter 1, on the Si(100) surface exclusively occurs on the (3x1) dihydride/monohydride domains which can be built up by H adsorption even in the temperature range for β_2 TD. [11,14,15] The fast AID on Si(100) was related to a local phase

transition from a (1x1) dihydride phase to a (3x1) dihydride/monohydride phase on the (2x1) monohydride surface. On the other hand, the slow AID was related to a phase transition from a (3x1) dihydride/monohydride phase to a (2x1) monohydride phase. We invoke the same mechanism, i.e., the AID on the Si(110) surface also occurs at such a site where β_2 TD can occur. A possible kinetic mechanism to reconcile the fourth-order rate law is such that an incident H atom break a Si–Si bond of –DSi–SiD– unit in a zigzag Si chain, of which adjacent sites are occupied with a dideuteride (see Fig.3.13), i.e.,

H + -DSiD—DSi—SiD- → -DSiD—DSiH— ·SiD-.

Sticking of an H atom to the monodeuteride results a locally high density of dihydrides (dideuterides). If such a local system with excessively high density dihydrides is thermodynamically unstable, it returns to the original phase by emitting a molecule. This process could give rise to the fast AID. If the temperature is, in contrast, low enough that such high density dihydride phase is thermodynamically stable, the fast AID cannot result. This is indeed recognized in the no occurrence of AID at 373 K as described in the previous subsection.

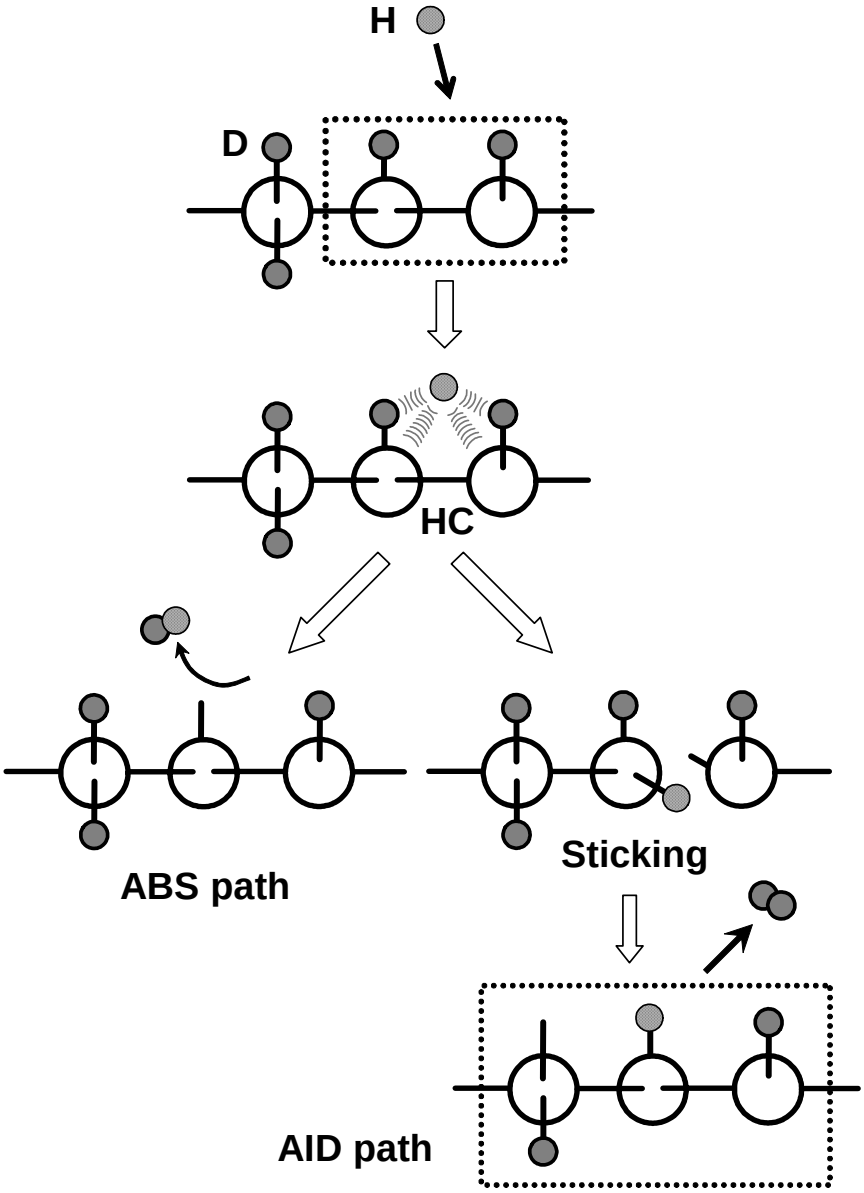

Fig. 3.13 Schematic illustration of the hot complex (HC) mediated ABS and AID mechanism. The D/Si(110) configuration is drawn (side view) at the top for the mixed phase with di- and monodeuterides. An incident H atom is bounded in chemisorption potential to form HC. The cell of the HC consists of a pair of adjacent –Di–Si– unit in a zigzag Si chain. The H atom of the HC interacts with neighboring D adatoms as well as Si atoms (second from the top). During energy relaxation, the H atoms abstract a nearby D adatom to generate HD ABS (second left from the bottom). Breaking the Si–Si bond in the zigzag chain or the backbond is an alternative energy relaxation path of the HC(second right from the bottom). It results in locally high density of dideuterides, from which a D_2 molecule is emitted, generating the fast AID (bottom).

The activation energy for the fast AID does not necessarily mean that it stems from the D_2 desorption process but rather means that it comes from the H sticking process to monodeuterides.[10] In this context, somewhat larger activation energy of 0.43 eV evaluated in the previous subsection may suggest that sticking to Si monodeuterides on the zigzag Si chains is more difficult in comparison to the Si(100) surfaces. This could be caused by the less strained zigzag Si chains compared with the highly stressed Si dimer bonds on the Si(100) surfaces.

The slow AID may be related to β_2 TD.[14,15] The β_2 peak appeared in Fig. 3.2 is a bit smaller in its intensity in comparison to the Si(100) surface. On the Si(110) surface, if it is related to such a conventional β_2 TD, the slow AID may be less efficient in comparison to the Si(100) surface. The observed second-order rate law suggests that β_2 TD requires diffusion of dihydrides along or across the zigzag Si chains to make an adjacent pair of dihydrides. To date, however, detailed mechanism of β_2 TD has not been revealed, yet. Particularly, local configuration of dihydrides that is responsible for β_2 TD is unclear. In order to completely understand the mechanism of slow AID we have to wait for more detailed knowledge on the β_2 TD on the Si(110) surface.

3.8 Conclusion

I studied the reactions of H(D) atoms with the Si(110) surface. IR and TD spectra showed presence of dideuterides as well as monodeuterides. I measured D abstraction by H atoms on the D-saturated and unsaturated Si(110) surfaces for various temperatures. HD and D_2 molecules were recognized as abstracted products. The HD molecules were produced either by a direct abstraction (ABS) or by an adsorption-induced desorption (AID), while D_2 molecules were produced exclusively through the AID path. The ABS was governed by a second-order rate law in θ_D. On the other hand, the AID followed a fourth-order rate law in θ_D. Even in the HD desorption, AID channels were involved because of coadsorption of D and H adatoms during exposure. I find that AID is promoted by dideuterides, suggesting that dideuterides (dihydrides) play an essential role in AID. Hence, the kinetics of the abstraction reactions on the Si(110) surfaces looked similar to those on the Si(100) surface. The measured HD and D_2 rate curves were analyzed with rate equations that include a second-order ABS and three fourth-order AID terms. I measured a time response of the HD and D_2 desorptions under the surface exposure to a pulsed H beam. I found that the HD ABS is prompt, but the D_2 AID consists of a slow process as well as a prompt one. Possible kinetic mechanisms for ABS and AID on the Si(110) surface were comparatively discussed with those on the Si(100) surface.

References

1. C. Lutterloh, A. Dinger, J. Kuppers, Surf. Sci. 482–485 (2001) 233.
2. Y. Tsukidate, M. Suemitsu, Jpn. J. Appl. Phys.40 (2001) 5206.
3. M. Shinohara, T. Kuwano, Y. Akama, Y. Kimura, M. Niwano, H. Ishida, R. Hatakeyama, J. Vac. Sci. Technol. A 21 (2003) 25.
4. P. Jacob, Y.J. Chabal, J. Chem. Phys. 95 (1991) 2897.
5. H. Kim, N. Taylor, T. Spila, G. Glass, S.Y. Park, J.E. Greene, J.R. Abelson, Surf. Sci. Lett. 380 (1997) L496.
6. C. Lutterloh, A. Dinger, J. Kuppers, Surf. Sci. 482–485 (2001) 233.
7. F. Khanom, S. Shimokawa, S. Inanaga, A. Namiki, M.N. Gamo, T. Ando, J. Chem. Phys. 113 (2000) 3792.
8. E. Hayakawa, F. Khanom, T. Yoshifuku, S. Shimokawa, A. Namiki, T. Ando, Phys. Rev. B 65 (2001) 033405.
9. A. Kubo, Y. Ishii, M. Kitajima, J. Chem. Phys. 117 (2002) 11336.
10. F. Khanom, A. Aoki, F. Rahman, A. Namiki, Surf. Sci. 536 (2003) 191
11. F. Rahman, M. Kuroda, T. Kiyonaga, F. Khanom, H. Tsurumaki, S. Inanaga, A. Namiki, J. Chem. Phys. 121 (2004) 3221.
12. D.D. Koleske, S.M. Gates, B. Jackson, J. Chem. Phys. 101 (1994) 3301.
13. G. Lupke, N.H. Tolk, L.C. Feldman, J. Appl. Phys. 93 (2003) 2317.
14. S. Inanaga, H. Goto, A. Takeo, F. Rahman, F. Khanom, H. Tsurumaki, A. Namiki, Surf. Sci. 596 (2005) 82.
15. A.R. Khan, A. Takeo, S. Ueno, S. Inanaga, T. Yamauchi, Y. Narita, H. Tsurumaki, A. Namiki, Surf. Sci. 601 (2007) 1635.